Chin. J. Astron. Astrophys. Vol. 5 (2005), No. 4, 371–378
(*http://www.chjaa.org*)

Chinese Journal of
Astronomy and
Astrophysics

The Effect of Method of Constructing the Mass Distribution on Single Stellar Populations *

Feng-Hui Zhang, Li-Fang Li and Zhan-Wen Han

National Astronomical Observatories, Yunnan Observatory, Chinese Academy of Sciences, Kunming 650011; *gssephd@public.km.yn.cn*

Received 2005 January 5; accepted 2005 April 8

Abstract We use two methods of constructing the initial mass distribution, the traditional way and Monte Carlo simulation, to obtain integrated $U-B$, $B-V$, $V-R$ and $V-I$ colours and absorption-line indices defined by the Lick Observatory image dissector scanner (referred to as Lick/IDS), for instantaneous burst solar-metallicity single stellar populations with ages in the range 1–15 Gyr. We find that the evolutionary curves of all colours obtained by the traditional method are smoother than those by Monte Carlo simulation, that the $U-B$ and $B-V$ colours obtained by the two methods agree with one another, while the $V-R$ and $V-I$ colours by the traditional method are bluer than those by Monte Carlo simulation. A comparison of the Lick/IDS absorption-line indices shows that the variations in all the indices by the traditional method are smoother than that for the Monte Carlo simulation, and that all the indices except for TiO_1 and TiO_2 are consistent with those for the Monte Carlo simulation.

Key words: star: evolution — galaxies: star clusters — galaxies: stellar content

1 INTRODUCTION

Amongst the distinct methods available for the study of the integrated light of stellar populations it is the method of evolutionary population synthesis (EPS) (first introduced by Tinsley 1968) that offers the most direct approach for modelling galaxies. Remarkable progress in this field has been made during the past decades.

Single stellar populations (SSPs) are assemblies of chemically homogeneous and coeval stars, and the history of star formation of any stellar system can be described by a superposition of SSPs of different ages and metallicities. SSPs thus help us to understand the evolution of clusters and galaxies (e.g., Gu et al. 2003; Zhou et al. 2005), hence the large number of researchers work in this field. We also studied instantaneous SSPs using the EPS technique (Zhang et al. 2002, 2004); in this kind of work the traditional way was used to construct the initial mass distribution

* Supported by the National Natural Science Foundation of China.

of SSPs. To investigate the effect of the method of constructing the initial mass distribution on the results we also used the Monte-Carlo technique.

In the traditional population synthesis we select for a sample, stars that are distributed evenly along the isochrone of SSP at a given age and the number of stars of a given mass is inferred from the assumed initial mass function (IMF). In the Monte-Carlo-simulations, we use a random-number generator in combination with the initial mass distribution function to produce the initial mass of stars, and the number of stars of a given initial mass is set equal to 1.

2 MODEL DESCRIPTION

In this study, we consider only different methods of constructing the initial mass distribution of SSPs, while the input physics (the stellar evolutionary models, stellar spectral library and the approach of obtaining the Lick/IDS indices) and the other model input parameters (the lower and upper mass cut-offs, the relative age of SSP and the metallicity of stars) are all the same, and so is the algorithm.

2.1 Initialization of SSPs

In the traditional EPS, we first give the masses of stars at the end-points of the various evolutionary phases, i.e., $M_{\rm hook}$ (the initial mass above which a hook appears in the main-sequence [MS]), $M_{\rm BGB}$ (the mass at the base of the giant branch [GB]), $M_{\rm TGB}$ (the mass at the tip of the GB), $M_{\rm BAGB}$ (the mass at the base of the asymptotic giant branch [AGB] or the end of the core helium burning [CHeB]), $M_{\rm STPAGB}$ (the mass at the start of the thermal pulsing asymptotic giant branch [TPAGB]) and $M_{\rm SFS}$ (the mass at the start of the final stages). Values for these masses are estimated from the detailed models of solar metallicity. Then, we select stars in equal mass interval within each evolutionary phase. The number of stars are given by the IMF. In this work we adopt the IMF of Kroupa, Tout & Gilmore (1993, hereafter KTG93), described by

$$\phi(M) = {\rm A}\cdot\begin{cases} 0.035M^{-1.3} & \text{if } \ 0.08 \le M < 0.5, \\ 0.019M^{-2.2} & \text{if } \ 0.5 \le M < 1.0, \\ 0.019M^{-2.7} & \text{if } \ 1.0 \le M < \infty, \end{cases} \tag{1}$$

where A is a normalization constant and M is the stellar mass in solar units. When normalizing the mass of an SSP to 1 $M_\odot$, i.e., $\int_{M_{\rm l}}^{M_{\rm u}} \phi(M) M {\rm d}M = 1$, and taking the lower and upper limits, $M_{\rm l}$ and $M_{\rm u}$, of the stellar mass range as 0.1 and 100 $M_\odot$, respectively, we obtain the normalization constants ${\rm A} \simeq 16.40$.

For Monte-Carlo-simulation the mass of star is chosen with the approximation to the IMF of Kroupa, Tout & Gilmore (1990, hereafter KTG90) as given by Kroupa, Gilmore & Tout (1991, hereafter KGT91),

$$M = 0.33\Big[\frac{1}{(1-X)^{0.75}+0.04(1-X)^{0.25}} - \frac{(1-X)^2}{1.04}\Big], \tag{2}$$

where X is a random variable uniformly distributed in the range [0,1]. Figure 1 illustrates two of the IMF used in this work.

2.2 Input Physics, Model Input and Algorithm

We use the stellar evolutionary models of Pols et al. (1998) obtained with the Eggleton stellar evolutionary code (Eggleton 1971, 1972, 1973; Han, Podsiadlowski & Eggleton 1994; Pols et al. 1995), the empirical and semi-empirical calibrated BaSeL-2.0 stellar spectral library of Lejeune,

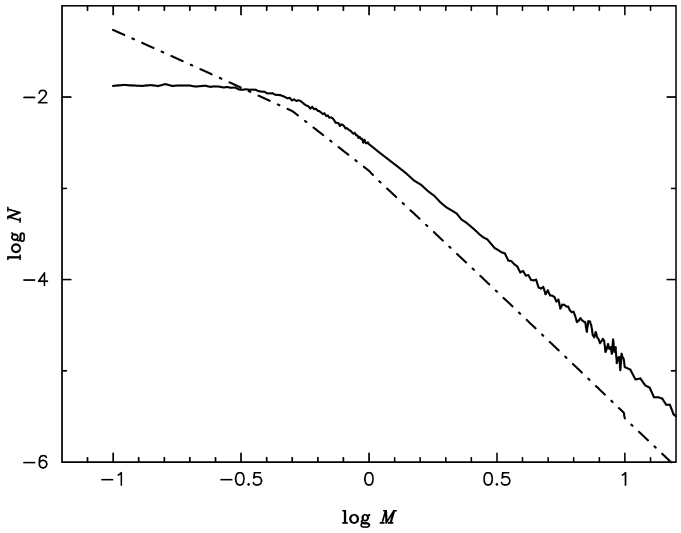

Fig. 1 Mass distribution of stars given by the KTG93 IMF (dot-dashed line) and the approximation to the IMF of KTG90 (solid line), obtained by a Monte Carlo process.

Cuisinier & Buser (1997, 1998) and the empirical fitting functions of Worthey et al. (1994). The evolutionary models of Pols et al. (1998) have been given in the convenient form of the rapid single stellar star evolution (SSE) package presented by Hurley, Pols & Tout (2000). Detailed descriptions of the stellar evolutionary models of Pols et al. (1998), the SSE package of Hurley et al. (2000) and the BaSeL-2.0 stellar spectra library of Lejeune et al. (1997, 1998) have been presented in Zhang et al. (2002), and the description of the empirical fitting functions of Worthey et al. (1994) has been given in Zhang et al. (2004), so we do not discuss them here. We refer interested readers to them.

In this work the relative age, τ, of SSP is assigned within the range of 1–15 Gyr, the solar metallicity is chosen, and the Reimers' mass-loss coefficient factor η is taken to 0.3.

Once the initial state of a single star (the mass M and metallicity Z) and the input physics data base are given, we can use the SSE algorithm to evolve a star in the SSP to an age of τ to give us the evolutionary parameters including the luminosity L, temperature $T_{\rm eff}$, radius R and current mass M_t. Next we use the BaSeL-2.0 stellar spectra to transform the evolutionary parameters to colours and stellar flux and then use the empirical fitting functions of Worthey et al. (1994) to derive the spectral absorption feature indices in the Lick/IDS system. Finally, using the equations given in Zhang et al. (2000, 2004) we can obtain the integrated colours, monochromatic flux and absorption feature indices for an instantaneous SSP of a particular age and metallicity.

3 RESULTS

We have constructed two distinct SSPs in order to investigate the effect of the method of constructing the initial mass distribution of SSPs on the integrated colours and Lick/IDS absorption indices for instantaneous burst solar-metallicity SSPs with ages in the range $1 \leq \tau \leq 15$ Gyr:

Model A uses the traditional way whereas Model B uses Monte-Carlo-simulation. For Model B, 2×10^6 stars are evolved.

In Figs. 2 and 3 we show the distribution of stars in the theoretical colour-magnitude diagram (CMD) for Models A and B at ages 1 Gyr and 13 Gyr. We see clearly that the distributions for the two models are significantly different. For Model A the stars within each evolutionary stage are evenly dispersed, while for Model B only the stars in the MS, Hertzsprung gap (HG) and CHeB stages are evenly distributed, the stars on the luminous GB and EAGB stages are scarce, and no or few stars exist on the thermally pulsing giant branch/proto planetary nebulae/planetary nebula phases, collectively known as the 'post EAGB' (PEAGB) phase. The reason that there are few luminous GB and EAGB stars and a total absence of PEAGB stars in our 2×10^6 sample is that the evolutionary time-scale of these stars is so short compared with that of MS stars. These differences in the distribution of stars are responsible for differences in the appearance of the EPS models. The absence of PEAGB stars will cause the disagreement of the integrated spectral energy distributions (ISEDs) in the ultra violet (UV) passbands (see the fraction contributions of different evolutionary stages to the ISEDs in figs. 3 and 4 of Zhang et al. 2004), the ISED for Model A is bluer than that for Model B in the UV range (Similar to the top panels of figs. 3 and 4 of Zhang et al. 2004). The rareness of luminous EAGB stars will lead to relatively large errors of the ISED in the infra-red (IR) and radio passbands because these stars make large contributions in these bands (see figs. 3 and 4 of Zhang et al. 2004).

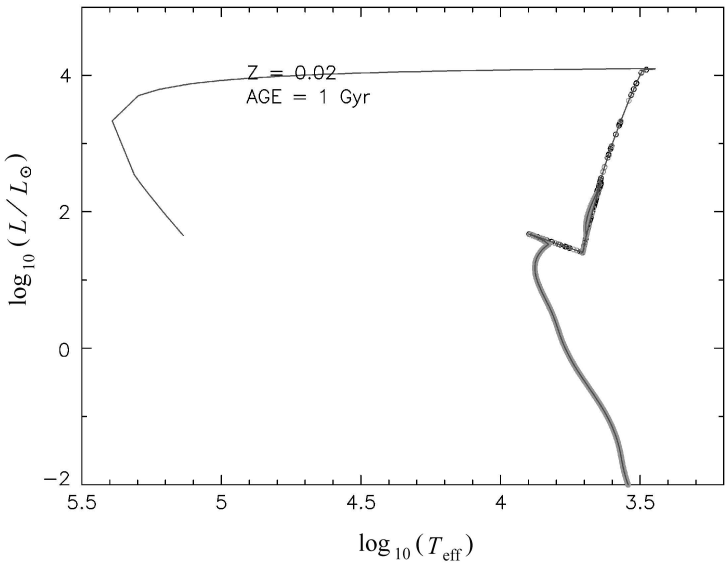

Fig. 2 Theoretical isochrones for SSPs with solar metallicity at age of 1 Gyr. Line represents Model A and points, Model B.

3.1 Colours

In Fig. 4 we give a comparison of the integrated $U-B$, $B-V$, $V-R$ and $V-I$ colours between Models A and B. We see that the evolutionary curves of these colours for Model A are smoother

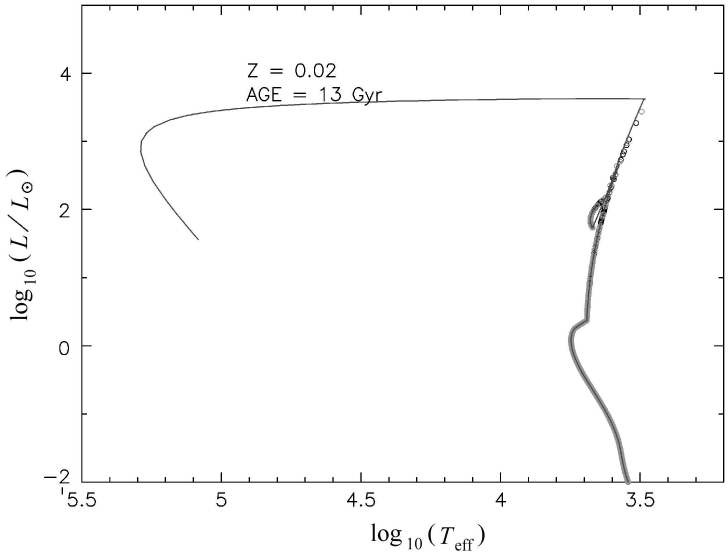

Fig. 3 Same as Figure 2, but for 13 Gyr.

than those for Model B. The integrated $U-B$, $B-V$ and $V-R$ colours for Model B fluctuate around those for Model A within a range of 0.05 mag, while the integrated $V-I$ colour for Model B is redder than that for Model B. In this paper we could not give the comparison of the redder colours (such as, $J-K$, $H-K$, etc.) because these colours for Model B have relatively large errors due to the small number statistics of PEAGB stars (see the discussion of Zhang et al. 2005) resulting in unsmooth evolutionary curves; while for Model A these redder colours vary smoothly. So we suggest that the integrated colours of Model A are preferable to those of Model B.

For comparison, we also present in Fig. 4 the integrated colours obtained by Bruzual & Charlot (2003, hereafter BC03). It shows that compared to BC03, our $U-B$ colour is bluer at early and intermediate ages, and redder at late age. Our $B-V$ colour agrees with BC03 at early age, while redder at intermediate and late ages. Our $V-R$ and $V-I$ colours are bluer than BC03 in all ages.

The data of BC03 we used are computed from the SSP model, in which are used the IMF of Salpeter (1955) with a slope of $\alpha = 2.35$ with lower and upper mass cutoffs $M_{\rm l} = 0.1\,M_{\odot}$ and $M_{\rm u} = 100\,M_{\odot}$, Padova (1994)'s stellar evolutionary tracks and BaSeL3.1 spectral library (low resolution). Differences between our models and BC03 can possibly be attributed to either the choice of stellar evolutionary models, the spectral library and/or the IMF.

3.2 Lick/IDS Indices

In Fig. 5 we show the evolution of Lick/IDS spectral absorption feature indices for Models A and B. We see that, again, the variation of all the indices is smoother for Model A than for Model B, and for all indices except for TiO_1 and TiO_2 the two models agree. For TiO_1 and TiO_2 the indices are bluer for Model A than for Model B. The analysis of this part indicates that the data of all Lick/IDS indices except for TiO_1 and TiO_2 can be safely used.

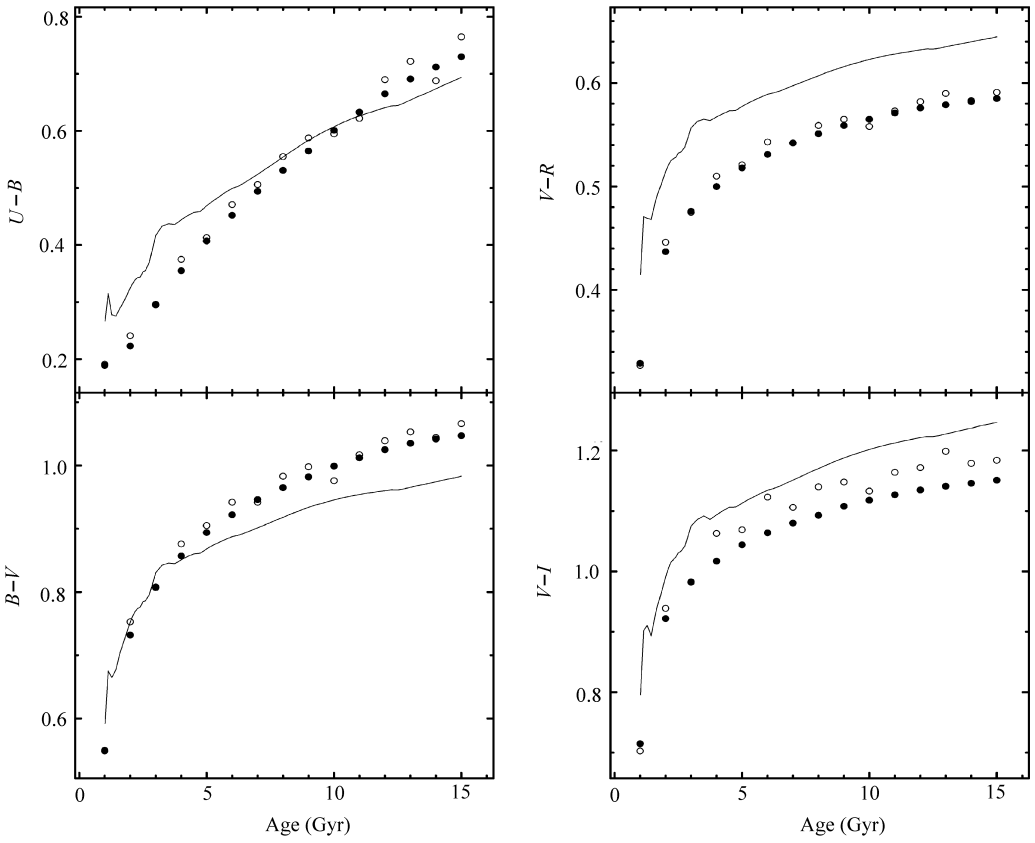

Fig. 4 Integrated colours as a function of age for solar-metallicity instantaneous burst SSPs. The solid circle represents Model A and open circle represents Model B. Also shown are the data of Bruzual & Charlot (2003, solid line).

In Fig. 5 we also present the Lick/IDS spectral absorption indices of BC03. It shows that our Ca4277, Mg_1, Mg_2, Mg_b, Fe 5335, Fe 5406, NaD, TiO_1 and TiO_2 indices are bluer than those of BC03 in all instances, our CN_1, CN_2, Fe 5709 and Fe 5782 indices are bluer than BC03 at early age, while redder at intermediate and late ages. The other indices G4300, Fe 4383, Ca4455, Fe 4531, Fe 4668, H_β, Fe 5015 and Fe 5270 indices obtained by us are bluer than those of BC03 at early age, while agreeing with them at intermediate and late ages.

4 SUMMARY AND CONCLUSIONS

We present integrated $U-B$, $B-V$, $V-R$ and $V-I$ colours and Lick/IDS absorption-line indices using two methods of constructing the initial mass distribution, by the traditional way and by Monte-Carlo-simulation, for instantaneous burst solar-metallicity single stellar populations with ages in the range 1–15 Gyr. A comparison of the integrated colours and Lick/IDS indices shows that the evolutionary curves for the traditional way are smoother than those for Monte-Carlo-simulation, that the $U-B$, $B-V$ colours and all indices except for TiO_1 and TiO_2

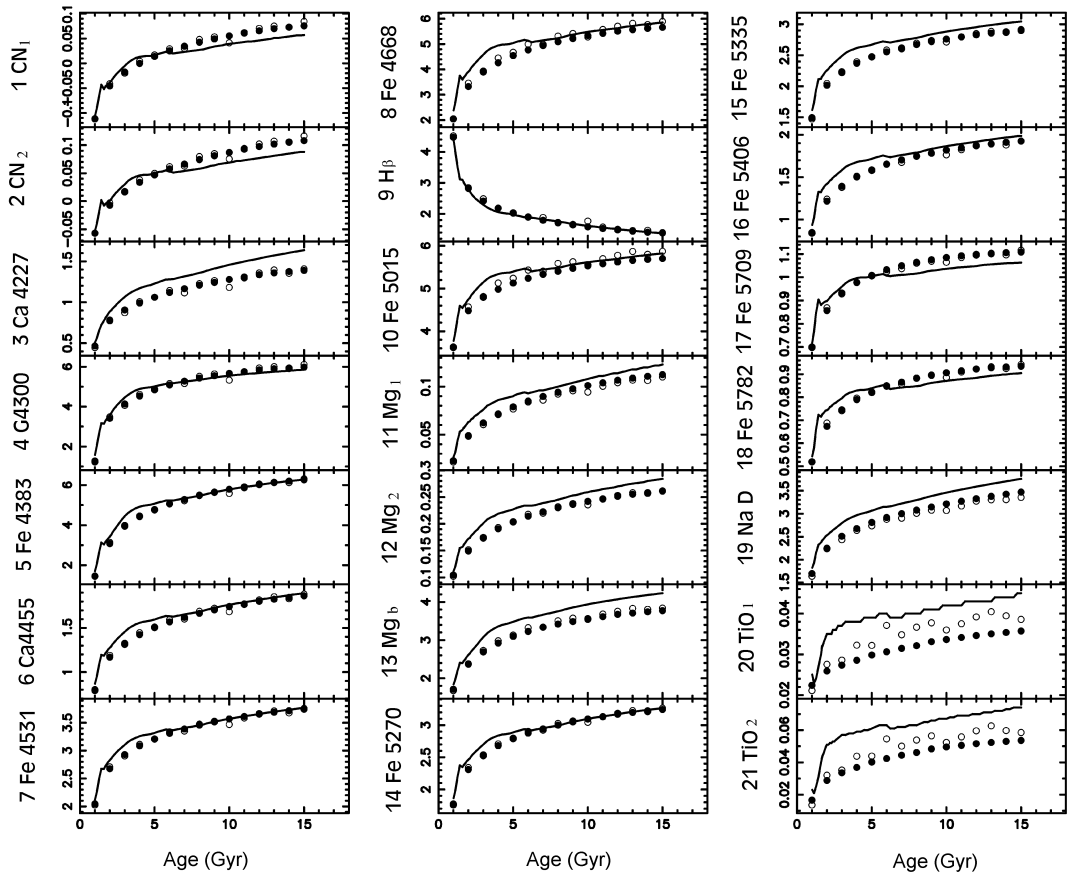

Fig. 5 Evolution of absorption indices in the Lick/IDS system for solar-metallicity instantaneous burst SSPs. The solid circle represents Model A and open circle represents Model B. Also shown are data of Bruzual & Charlot (2003, solid line).

for the traditional way agree with the Monte-Carlo-simulation, while the $V-R$ and $V-I$ colours present larger discrepancies. Because the Monte Carlo simulation only had few stars on some important evolutionary stages, we suggest that the traditional way should be used when constructing the initial mass distribution for single stellar populations.

Acknowledgements This work was funded by the National Natural Science Foundation of China (Grant Nos 10303006, 19925312 & 10273020), by the Chinese Academy of Sciences (KJCX2-SW-T06) and by the 973 scheme (NKBRSF G1999075406).

References

Bruzual G., Charlot S., 2003, MNRAS, 344, 1000
Eggleton P. P., 1971, MNRAS, 151, 351
Eggleton P. P., 1972, MNRAS, 156, 361
Eggleton P. P., 1973, MNRAS, 163, 279
Gu Q., Shi L., Lei S., Liu W., Huang J., 2003, Chin. J. Astron. Astrophys. (ChJAA), 3, 203
Han Z., Podsiadlowski P., Eggleton P. P., 1994, MNRAS, 270, 121
Hurley J. R., Pols O. R., Tout C. A., 2000, MNRAS, 315, 543
Kroupa P., Tout C. A., Gilmore G., 1990, MNRAS, 244, 76
Kroupa P., Gilmore G., Tout C. A., 1991, MNRAS, 251, 293
Kroupa P., Tout C. A., Gilmore G., 1993, MNRAS, 262, 545
Lejeune T., Cuisinier F., Buser R., 1997, A&AS, 125, 229
Lejeune T., Cuisinier F., Buser R., 1998, A&AS, 130, 65
Pols O. R., Schröder K. P., Hurley J. R., Tout C. A., Eggleton P. P., 1998, MNRAS, 298, 525
Pols O. R., Tout C. A., Eggleton P. P., Han Z., 1995, MNRAS, 274, 964
Salpeter E. E., 1955, ApJ, 121, 161
Tinsley B. M., 1968, ApJ, 151, 547
Worthey G., Faber S. M., Gonzalez, J. J., Burstein, D., 1994, ApJS, 94,687
Zhang F., Han Z., Li L., Hurley J. R., 2002, MNRAS, 334, 833
Zhang F., Han Z., Li L., Hurley J. R., 2004, MNRAS, 350, 710
Zhang F., Han Z., Li L., Hurley J. R., 2005, MNRAS, 357, 1088
Zhou H., Wang T., Dong X., Li C., Zhang X., 2005, Chin. J. Astron. Astrophys. (ChJAA), 5, 41